Supplement of

Long-term positive trend in the mass term of global atmospheric angular momentum and its relationships with the moistening of the equatorial atmosphere

Wirid Birastri[1,2], Tri Wahyu Hadi[3], Nining Sari Ningsih[4], Faiz Rohman Fajary[3]

[1]Doctoral Program in Earth Sciences, Bandung Institute of Technology, Bandung, Indonesia.

[2]Atmospheric Science Research Group, Institut Teknologi Sumatera, South Lampung, Indonesia.

[3]Atmospheric Science Research Group, Bandung Institute of Technology, Bandung, Indonesia.

[4]Applied and Environmental Oceanography Research Group Research Group, Bandung Institute of Technology, Bandung, Indonesia.

Table S1 Data used in the process of water vapor data evaluation

Data	Variable	Spasial resolution	Temporal resolution	Period	Data source
AQUA/ AIRS	Total integrated column water vapor burden (ascending/ descending)	1° x 1°	monthly	2003-2020	https://acdisc.gesdisc.eosdis.nasa.gov/data/Aqua_AIRS_Level3/AIRS3STD.7.0/
ERA5	Total column vertically-integrated water vapour	0.25° x 0.25°	monthly	1959-2010	https://cds.climate.copernicus.eu/cdsapp#!/dataset/reanalysis-era5-pressure-levels?tab=overview#!%2Fdataset%2Freanalysis-era5-single-levels%3Ftab=form
ERA-20C	Total column vertically-integrated water vapour	0.25° x 0.25°	monthly	1950-2010	https://apps.ecmwf.int/datasets/data/era20c-daily/levtype=sfc/type=an/. The Public Datasets Service for this dataset closed on 1 June 2023.
JRA55	Precipitable water	1.25° x 1.25°	6-hourly converted to monthly	1958-2020	https://rda.ucar.edu/datasets/ds628.1/dataaccess/
NCEP/ NCAR (R1)	Precipitable water	2.5° x 2.5°	daily converted to monthly	1950-2020	https://downloads.psl.noaa.gov/Datasets/ncep.reanalysis/Dailies/surface/

Table S2 Root Mean Square Difference (RMSD) and correlation coefficient calculated between AQUA/AIRS and four reanalysis water vapor datasets (ERA5, ERA-20C, JRA55, and NCEP) for each monthly mean (M), monthly mean anomaly (MA), annual mean (A), and annual mean anomaly (AA) for the period of 2003-2020. Anomalies are deviations of total water vapor from its long-period average value for each domain: Global, equatorial belt (EQ), northern (NH), and southern hemisphere (SH).

	Global				**EQ**				**NH**				**SH**				
ERA5	1.64	1.35	1.50	1.23	1.90	0.68	1.84	0.57	0.45	0.44	0.36	0.36	1.03	0.36	0.99	0.32	
ERA-20C	6.19	1.21	6.10	0.87	4.93	0.71	4.86	0.40	1.86	0.41	1.69	0.25	0.61	0.36	0.56	0.29	
JRA55	2.50	1.34	2.39	1.21	2.14	0.74	2.06	0.64	14.77	0.51	3.21	0.28	14.45	0.63	3.14	0.48	RMSD
NCEP	2.35	1.51	2.02	1.26	2.53	0.93	2.16	0.71	1.58	0.38	1.00	0.27	1.49	0.39	1.46	0.34	
ERA5	0.97	0.70	0.66	0.66	0.91	0.86	0.82	0.82	1.00	0.68	0.69	0.69	0.99	0.45	-0.05	-0.05	
ERA-20C	0.97	0.62	0.49	0.58	0.84	0.79	0.72	0.83	1.00	0.56	0.47	0.49	1.00	0.42	-0.07	0.04	Correlation
JRA55	0.97	0.65	0.59	0.59	0.88	0.82	0.75	0.75	-0.94	0.11	0.30	0.30	-0.94	-0.14	-0.27	-0.27	coef.
NCEP	0.95	0.60	0.59	0.59	0.60	0.74	0.71	0.71	1.00	0.66	0.72	0.72	0.99	0.31	-0.17	-0.17	
	M	MA	A	AA	M	MA	A	AA	M	MA	A	AA	M	MA	A	AA	

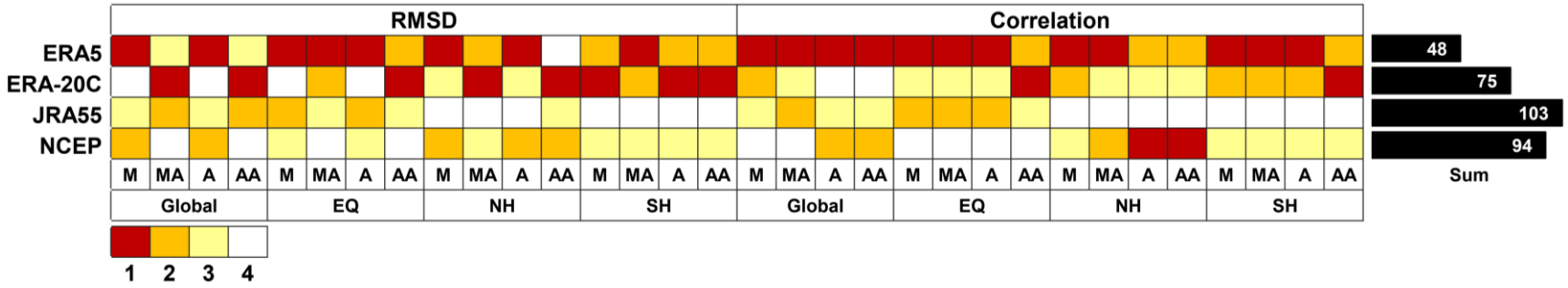

Fig. S1 Heatmap of the rank-based evaluation of water vapor datasets evaluation as shown in Table S2. Colors shadings indicates the rank of each performance metric among the four datasets rangin from 1 (best) to 4 (worst). The cumulative rank score for each dataset is shown as a bar chart on the right-hand side.

(a)

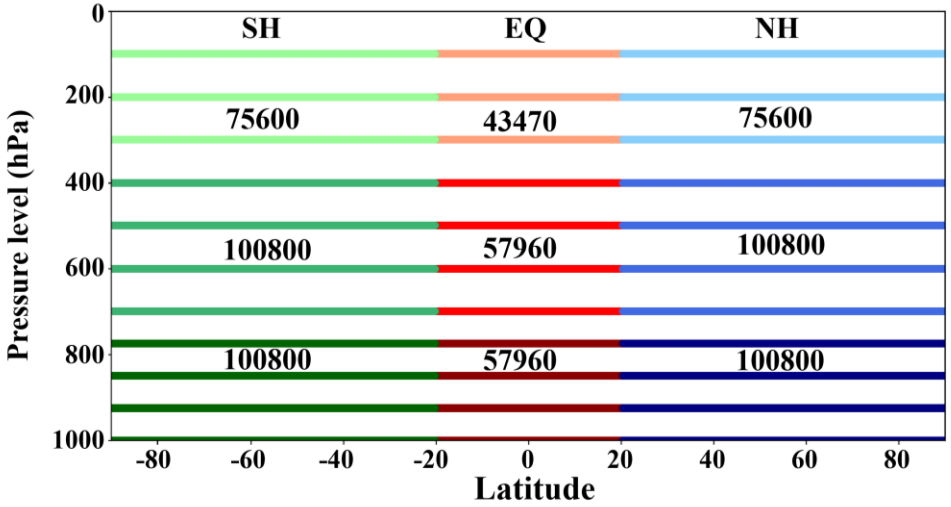

(b)

Data (ω, u, v)	**ERA5**
Spatial resolution	**0.25◦× 0.25◦**
Temporal resolution, time step simulation	**6-hourly**
Temporal resolution, model output	**daily**
Vertical level (hPa) data	**100,150,200,225,250,300,350, 400,450,500,550,600,650,700, 750,775,800,825,850,875,900, 925,950,975,1000**
Simulation period	**1969-1999**

(c)

Domain	**Latitude boundary (◦)**	**Longitude (◦)**	**Pressure level (hPa)**		
			lower	**middle**	**upper**
EQ	-20.00:0.25:20.00	0:4:360	775, 850, 925, 1000	400, 500, 600, 700	100, 200, 300
NH	-20.25:0.25:89.75				
SH	-20.25:0.25: -89.75				

Fig. S2 Simulation setup for the Lagrangian particle tracking model: (a) initial position of particle (color-coded) and the number of particles at $t = 0$ for each domain Equatorial (EQ), Northern Hemisphere(NH), and Southern Hemisphere (SH) and vertical level (lower, middle, and upper), (b) model configuration, including input datasets, spatial and temporal resolution of input data and model output, and simulation period. (c) Spatial definition of the particle domains, including initial longitude-latitude boundaries and vertical level groupings at the start of the simulation.

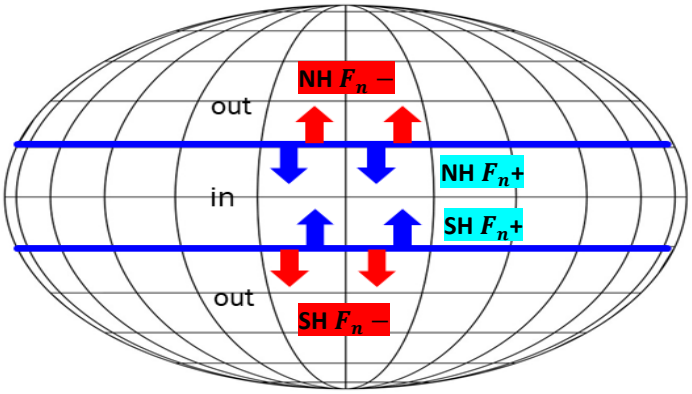

Fig. S3 Schematic illustration of the sign convenction used for the normalized boundary flux F_n. The blue horizontal lines denote the northern (NH) and southern (SH) equatorial boundaries across which the fluxes are evaluated. Positive (negative) values of F_n indicate particle transport into (out of) equatorial region across the NH and SH boundaries. Blue arrows denote equatorward transport, whereas red arrows indicate poleward transport. The labels $F_n +$ and $F_n -$ indicate positive and negative flux contribution at each boundary, respectively. This schematic is provided for conceptual clarity only and does not represent quantitative results.

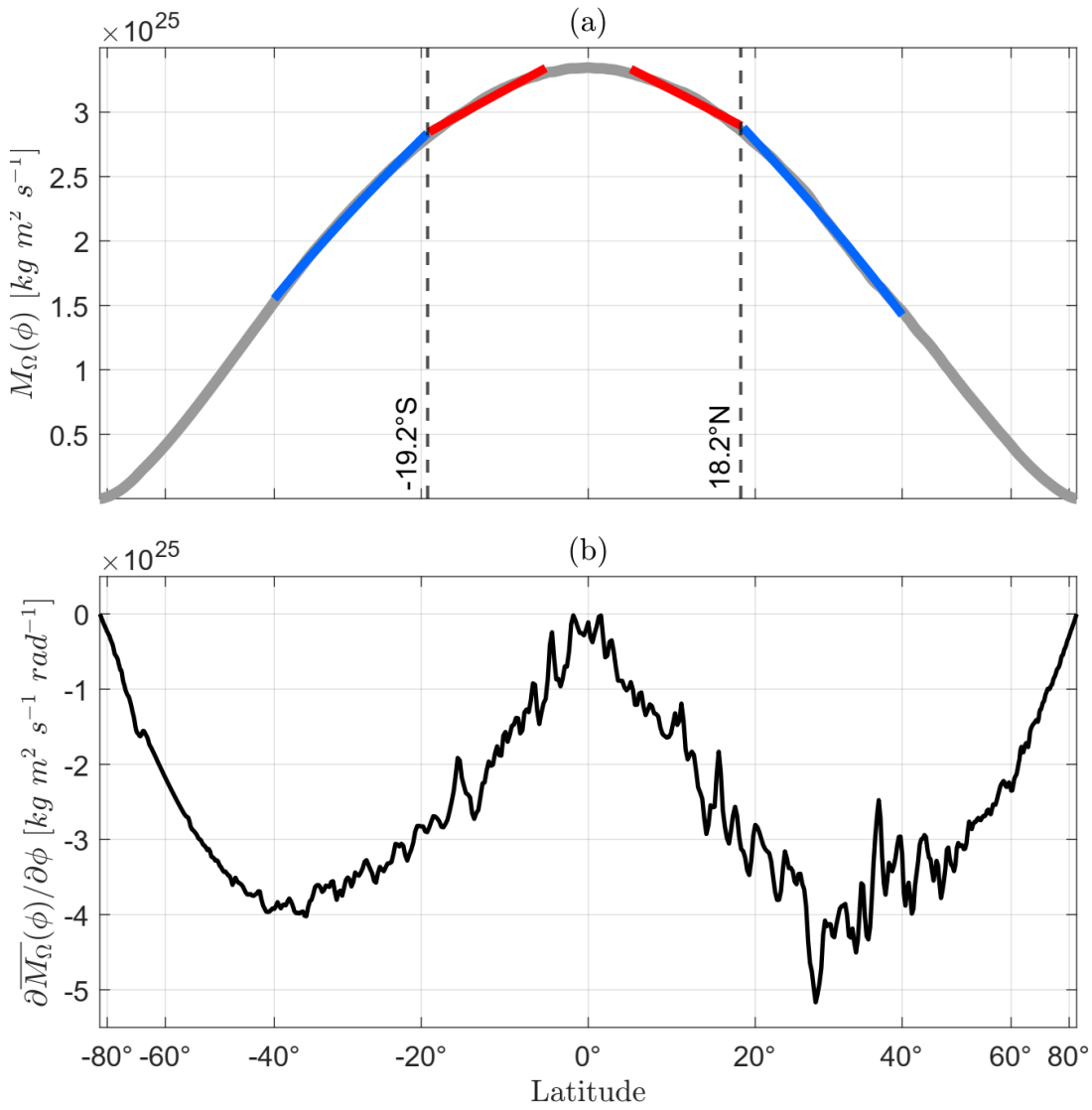

Fig. S4. (a) Latitudinal distribution of the time-mean zonally integrated monthly M_Ω, $\bar{M}_\Omega(\phi)$, computed from ERA5 reanalysis for 1959–2020. The red and blue lines denote the piecewise linear fits on the equatorial-side (tropical) and off-equatorial (subtropical) portions of the profile, respectively. The vertical dashed lines mark the change-point latitudes identified using constrained change-point detection (5° to 40°degree latitude). (b) Latitudinal gradient of $\bar{M}_\Omega(\phi)$, $\frac{\partial \bar{M}_\Omega(\phi)}{\partial \phi}$ evaluated separately from the EQ (0°) toward NH (40° N) and toward the SH (40° S).